A functional genetic screen identifies retinoic acid signaling as a target of histone deacetylase inhibitors

Mirjam T. Epping*, Liming Wang*†, Jane A. Plumb‡, Michele Lieb§, Hinrich Gronemeyer§, Robert Brown‡, and René Bernards*¶

*Division of Molecular Carcinogenesis and Center for Biomedical Genetics, The Netherlands Cancer Institute, Plesmanlaan 121, 1066 CX, Amsterdam, The Netherlands; ‡Centre for Oncology and Applied Pharmacology, University of Glasgow, Cancer Research United Kingdom Beatson Laboratories, Garscube Estate, Glasgow G61 1BD, United Kingdom; and §Department of Cell Biology and Signal Transduction, Institut de Genetique et de Biologie Moleculaire et Cellulaire/Centre National de la Recherche Scientifique/Institut National de la Santé et de la Recherche Médicale/Université Louis Pasteur, BP 163, 67404 Illkirch Cedex Strasbourg, France

Edited by Ed Harlow, Harvard Medical School, Boston, MA and approved September 24, 2007 (received for review March 17, 2007)

Understanding the pathways that are targeted by cancer drugs is instrumental for their rational use in a clinical setting. Inhibitors of histone deacetylases (HDACI) selectively inhibit proliferation of malignant cells and are used for the treatment of cancer, but their cancer selectivity is understood poorly. We conducted a functional genetic screen to address the mechanism(s) of action of HDACI. We report here that ectopic expression of two genes that act on retinoic acid (RA) signaling can cause resistance to growth arrest and apoptosis induced by HDACI of different chemical classes: the retinoic acid receptor α (RARα) and preferentially expressed antigen of melanoma (PRAME), a repressor of RA signaling. Treatment of cells with HDACI induced RA signaling, which was inhibited by RARα or PRAME expression. Conversely, RAR-deficient cells and PRAME-knockdown cells show enhanced sensitivity to HDACI *in vitro* and in mouse xenograft models. Finally, a combination of RA and HDACI acted synergistically to activate RA signaling and inhibit tumor growth. These experiments identify the RA pathway as a rate-limiting target of HDACI and suggest strategies to enhance the therapeutic efficacy of HDACI.

biomarker | chromatin modification | drug resistance | epigenetics | nuclear hormone receptor

Epigenetic DNA and histone modifications are appreciated as major determinants in the control of gene activity, and they are extensively deregulated in cancer. Histone acetylation is regulated by the opposing activities of histone acetyltransferases (HATs) and histone deacetylases (HDACs), which catalyze the addition and removal of acetyl groups to histones, respectively, and to a growing list of nonhistone substrates (1). The activities of HATs and HDACs are altered in several human cancers, and modulation of these classes of enzymes provides a potentially attractive therapeutic modality (2, 3). Several classes of HDAC inhibitors (HDACI) have been identified that block enzyme activity, resulting in global histone hyperacetylation. A wide array of literature on HDACI exists, describing their various effects, including G_1 and G_2/M cell cycle arrests, apoptosis, and differentiation, and several HDACI have entered clinical trials (2–4). Gene expression profiling studies revealed that HDACI treatment induces alterations in transcription of $<5\%$ to $\approx 20\%$ of expressed genes (5, 6) and have not elucidated a consistent picture of the pathway(s) or target(s) that are modulated by HDACI and, consequently, have not provided a comprehensive explanation for their anticancer effects.

To identify cellular targets of HDACI action in transformed cells, we used the approach of large-scale functional genetic screening. In this screen we asked which genes or pathways could confer cellular resistance to HDACI. The present work provides evidence that the retinoic acid receptor (RAR) pathway is targeted by HDACI and that the cytotoxic effects of HDACI in solid tumor cells are, at least in part, through derepression of retinoic acid (RA) signaling.

Results

Genetic Screen for HDACI Resistance Genes. To identify genes involved in HDACI resistance, we have conducted an unbiased functional genetic screen. The hydroxamate HDACI PXD101 was used to screen a high-complexity human cDNA expression library in p53-deficient mouse embryonic fibroblasts (MEFs) with an oncogenic Ras^{V12} gene (Ras^{V12} MEFs), which were used as a genetically well defined model for malignant cells. After infection of the cells with the retroviral cDNA library, cells were seeded at low density and were cultured in 1 μM PXD101. The majority of the infected cells ceased to proliferate and underwent apoptosis. A small number of surviving cells formed colonies despite continued exposure to PXD101, and these single colonies were picked and expanded for sequencing of the proviral inserts (Fig. 1*a*). The identified cDNAs in independent colonies encoded for RARα and the tumor antigen preferentially expressed antigen of melanoma (PRAME) (7). We cloned the wild-type cDNAs for RARα and PRAME and introduced them into Ras^{V12} MEFs and found that, indeed, these cDNAs conferred resistance to 1 μM PXD101 in colony formation assays (Fig. 1*b*). In proliferation assays, RARα- and PRAME-expressing cells continued to grow in the presence of 1 μM PXD101, whereas control cells were arrested (Fig. 1*c*). Low doses of HDACI induce growth arrest of solid tumors, and high doses induce apoptosis. The growth advantage of RARα and PRAME existed over a range of PXD101 concentrations (0.5–3 μM), including low doses with predominant growth arrest and high doses with growth arrest and apoptosis [see supporting information (SI) Fig. 6]. The intrinsic growth rate of Ras^{V12} MEFs was not affected by the introduction of *RARα* or *PRAME* because all cells proliferated equally fast in the absence of PXD101 treatment (Fig. 1*c*). To assess the effects of these genes on apoptosis, we measured caspase activity in cells exposed to a range of HDACI concentrations (0.1–10 μM). *RARα* and *PRAME* expression inhibited the induction of apoptosis by HDACI in a concentration-dependent manner (SI Fig. 6).

RARα and PRAME Inhibit HDACI-Induced RA Signaling. Cells with ectopic RARα and PRAME were not devoid of responses to

Author contributions: R. Bernards designed research; M.T.E., L.W., J.A.P., and M.L. performed research; H.G. and R. Brown contributed new reagents/analytic tools; M.T.E., L.W., J.A.P., R. Brown, and R. Bernards analyzed data; and M.T.E. and R. Bernards wrote the paper.

The authors declare no conflict of interest.

This article is a PNAS Direct Submission.

Freely available online through the PNAS open access option.

Abbreviations: AD, activation domain; HDAC, histone deacetylase; HDACI, HDAC inhibitor; KD, knockdown; luc, luciferase; MEF, mouse embryonic fibroblast; NR, nuclear receptor; PRAME, preferentially expressed antigen of melanoma; RA, retinoic acid; RAR, retinoic acid receptor; RARE, retinoic acid-responsive element; tk, thymidine kinase; TKO, triple knockout; SAHA, suberoylanilide hydroxamic acid; TSA, trichostatin A.

†Present address: Urology Department of Changzheng Hospital, Fengyang Road 415, 200003 Shanghai, People's Republic of China.

§To whom correspondence should be addressed. E-mail: R.Bernards@nki.nl.

This article contains supporting information online at www.pnas.org/cgi/content/full/0702518104/DC1.

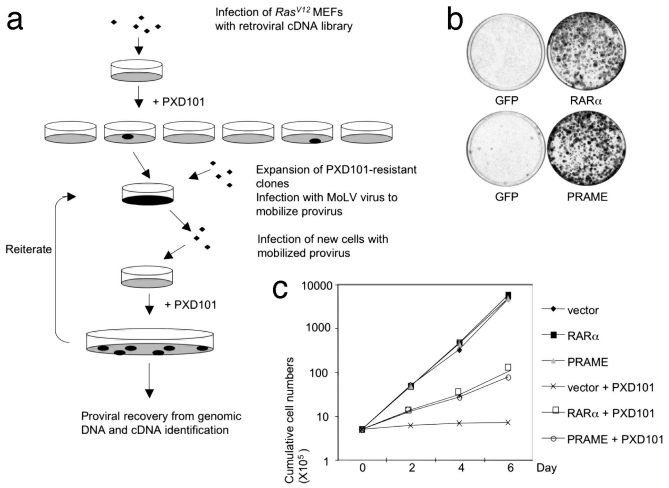

Fig. 1. Functional genetic screen to identify HDACI resistance genes. (*a*) Schematic outline of the genetic screen. A complex retroviral human cDNA library was introduced in oncogenic Ras^{V12}-transformed $p53^{-/-}$ MEFs (Ras^{V12} MEFs) and plated at low density. The cells were selected for growth in the continuous presence of 1 μM PXD101, and individual colonies were isolated after 3 weeks. Proviral insertions were mobilized by infection with wild-type Moloney leukemia virus (MoLV), and new cells were infected with the mobilized virus and subjected to a second round of selection in 1 μM PXD101. Proviral cDNA inserts in resistant colonies were recovered by PCR and sequenced. (*b*) In colony formation assays, Ras^{V12} MEFs were transduced with PRAME, RARα, or GFP (control) retrovirus, plated at low density, and treated with 1 μM PXD101. (*c*) Proliferation of Ras^{V12} MEFs with RARα or PRAME in the presence of 1 μM PXD101.

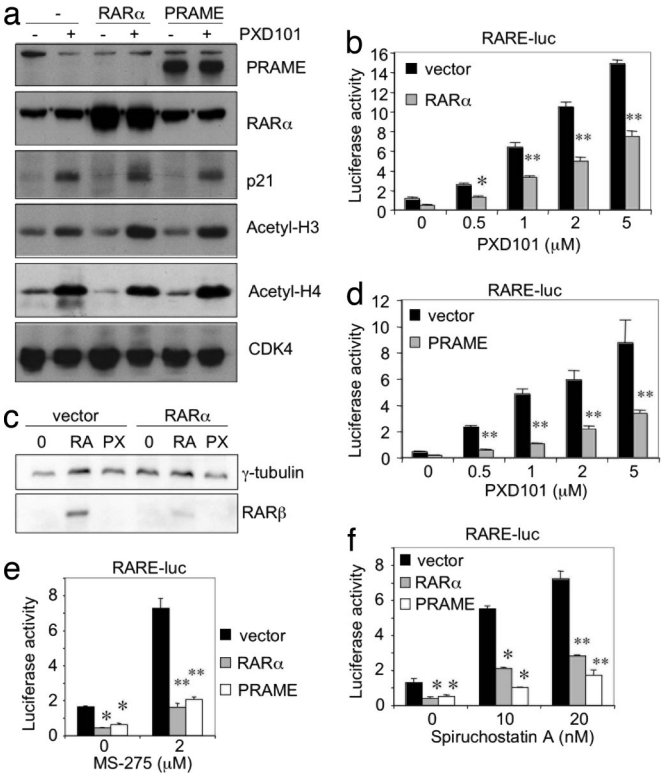

Fig. 2. RARα and PRAME inhibit RA signaling induced by HDACI. (*a*) Ras^{V12} MEFs were transduced with PRAME or RARα retroviruses and treated with 1 μM PXD101 for 16 h. Cell extracts were immunoblotted for acetyl-H3, acetyl-H4, p21, PRAME, RARα, and CDK4 (loading control). (*b* and *d–f*) RARα and PRAME inhibit HDACI-induced RA signaling. Ras^{V12} MEFs (*b* and *d*) and U2OS cells (*e* and *f*) were cotransfected with expression vectors for RARα and PRAME and the RARE-luc reporter, and the cells were treated with the indicated HDACI. *, $P < 0.05$; **, $P < 0.005$. (*c*) Immunoblot from cells treated with 1 μM RA or 1 μM PXD101 for 48 h showing the induction of RARβ.

PXD101 because acetylhistone H3 and H4 and $p21^{cip1}$ levels increased as expected upon treatment with 1 μM PXD101 (Fig. 2*a*). This result indicates that the identified cDNAs acted downstream of global histone hyperacetylation to rescue cells from HDACI-induced growth arrest. RARα is a member of the family of nuclear hormone receptors and is a dual transcription factor, which is bound to corepressor complexes in the absence of ligand but transactivates its target genes upon binding of RA (8). PRAME was recently described as a dominant repressor of RA signaling (9). Thus, the genetic screen described above identified two genes that act in the same pathway, raising the possibility that resistance to HDACI is connected to RA signaling. To test this connection, we transfected Ras^{V12} MEFs with a luciferase construct containing retinoic acid-responsive elements (RAREs; RARE3-tk-luc). Treatment of the cells with 0.5–5 μM PXD101 activated the reporter in a concentration-dependent manner, but expression of RARα attenuated the induction of RA signaling by PXD101 (Fig. 2*b*). Overexpression of RARα also inhibited the up-regulation of its direct target *RARβ* (16) by RA (Fig. 2*c*), which suggested that ectopically expressed RARα had acted as a transcriptional repressor in the screen. Similarly, PRAME blocked RA signaling induced by 0.5–5 μM PXD101 (Fig. 2*d*). These results raised the possibility that repression of the RA pathway is a mechanism of HDACI resistance and that derepression of the RA pathway is one of the mechanisms through which HDACI exert their anticancer activity.

HDACI of different chemical classes were tested for their effects on the RARα- and PRAME-expressing cells, including MS-275 (a benzamide), SAHA (a hydroxamic acid derivative), butyric acid (a small-chain fatty acid), and spiruchostatin A (a cyclic tetrapeptide with activities similar to FK-228/depsipeptide) (10). Exposure to these HDACI effectively arrested control cells, but Ras^{V12} MEFs with ectopic RARα and PRAME were able to grow to higher cell densities than were GFP controls (Fig. 3*c*). The effects of these HDACI on RA signaling were measured, and all were found to induce RAR transactivation, which could be blocked by *RARα* and *PRAME* expression (Fig. 2 *e* and *f* for MS-275 and spiruchostatin A, respectively). These observations indicate that the RA pathway is targeted by multiple HDACI, independent of structural class. The colony formation assays were then repeated with other commonly used chemotherapeutic drugs (cisplatin, 5-FU, bortezomib). As expected, these drugs caused concentration-dependent cell death, but RARα and PRAME did not confer resistance to any of these agents (SI Fig. 7). Thus, the protective effect of the RA pathway showed specificity for HDACI. Furthermore, both genes conferred resistance to PXD101 in a variety of cell lines from solid tumors (SI Fig. 8). The use of multiple cell lines and mouse models throughout this work suggests that the observed phenotypes are not restricted to a single cell line but have general validity. In a few cell lines with low endogenous RARα expression, PRAME expression did not rescue from HDACI, consistent with the notion that PRAME acts through RARα (9). When we coexpressed both genes in these cell lines, a higher level of HDACI resistance resulted than appeared with either gene alone (SI Fig. 8).

Resistance to HDACI Requires Repression of the RA Pathway. To investigate further the role of RA signaling in HDACI resistance, we used several mutants of RARα. The C-terminal ligand-binding domain of RARα contains a repression function and a ligand-dependent activation function AF-2 (11). The AF-2 activation domain (AD) core corresponds to the α-amphipathic helix H12, and its integrity is essential for the ligand-inducible activation of RAR (12, 13). The RARα-Rac mutant is an AF-2 AD core-deficient mutant caused by a small internal deletion, and RARα-

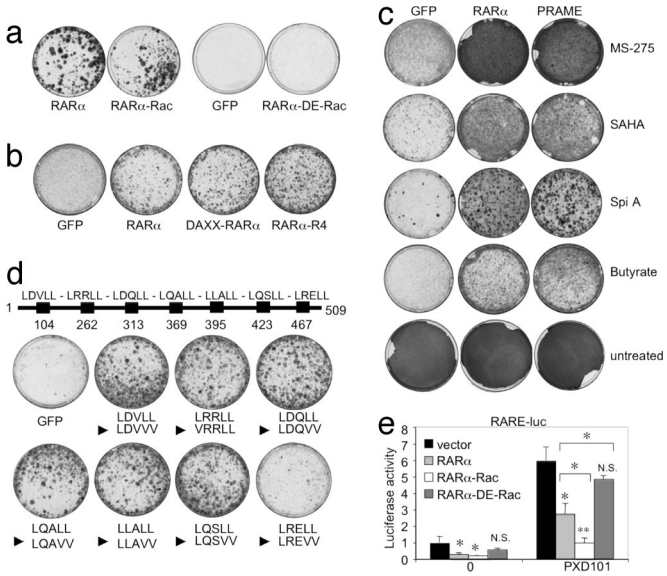

Fig. 3. Effects of RARα and PRAME expression on sensitivity to HDACI. (*a* and *b*) The repression function of RAR is sufficient for rescue from PXD101. *Ras*^{V12} MEFs were transduced with full-length RARα, mutants of RARα, or GFP (control) and were subsequently treated with 1 μM PXD101 in colony formation assays. (*c*) *Ras*^{V12} MEFs with RARα, PRAME, or GFP (control) expression were subjected to colony formation assays in 2 μM MS-275, 2 μM SAHA, 15 nM spiruchostatin A, or 2.5 mM butyrate. (*d*) Schematic representation of PRAME indicating seven putative NR boxes (LXXLL) with numbers indicating the first amino acid residue of each motif. PRAME NR box mutants were generated by replacement of leucines (L) by valines (V), and arrows indicate the mutant sequences. *Ras*^{V12} MEFs were transduced with retroviruses encoding these PRAME NR box mutants and treated with 1 μM PXD101 in colony formation assays. (e) RARα mutants were tested for their abilities to repress RA signaling in U2OS cells treated with 2 μM PXD101. *, $P < 0.05$; **, $P < 0.005$.

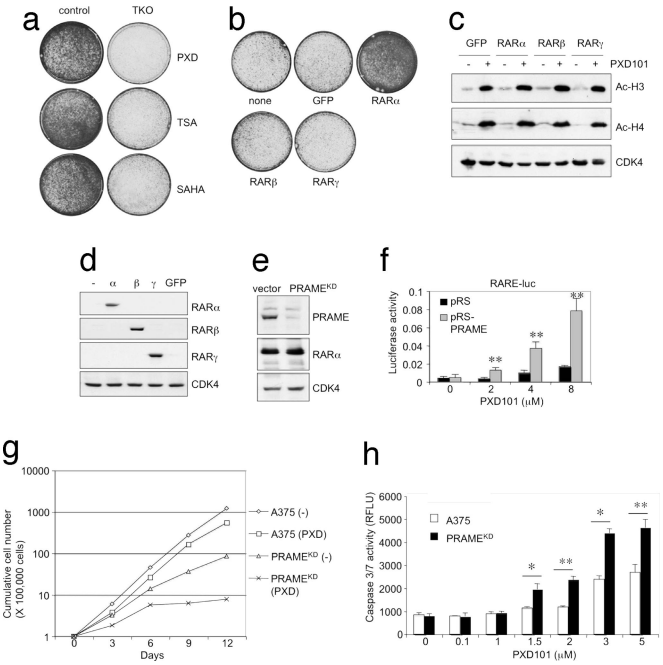

Fig. 4. RAR- and PRAME-deficient cells are sensitive to HDACI. (*a*) RARαβγ TKO MEFs and their matched controls were subjected to colony formation assays in the presence of 0.25 μM PXD101, 0.025 μM TSA, or 0.25 μg/ml SAHA. (*b*) Colony formation assays in 0.25 μM PXD101 with TKO MEFs after introduction of human RAR isoforms. (*c* and *d*) Western blots with lysates of TKO MEFs infected with retroviruses encoding human RAR isoforms or GFP (control) with or without treatment with 1 μM PXD101 for 16 h. (*e*) A375 melanoma cells were stably transfected with pRS-PRAME to knock down endogenous PRAME and are indicated as A375-PRAME^{KD} cells. (*f*) A375 cells were cotransfected with pRS-PRAME and the RARE-luc reporter and treated with PXD101. *, $P < 0.05$; **, $P < 0.005$. (*g*) Proliferation of A375 and A375-PRAME^{KD} cells in the presence of 0.25 μM PXD101. (*h*) Apoptosis was induced in A375 and A375-PRAME^{KD} cells by treatment with PXD101 for 24 h before detection of caspase 3/7 activity. *, $P < 0.05$; **, $P < 0.005$.

DE-Rac only comprises the ligand-binding domain of RARα and also lacks the AD core. RARα-Rac is a constitutive inhibitor of RAR transactivation, both in the presence and absence of RA. *Ras*^{V12} MEFs expressing wild-type RARα and RARα-Rac were able to proliferate and form colonies in the presence of 1 μM PXD101, but cells expressing RARα-DE-Rac failed to do so, most likely because of the lack of the DNA-binding domain (Fig. 3*a*). Consistent with this finding, RARα-Rac was able to repress RARE3-tk-luc reporter activity induced by PXD101, but RARα-DE-Rac was unable to do so (Fig. 3*e*). The RAR-R4 mutant is unable to bind ligand and was also able to rescue cells from PXD101-induced growth arrest and apoptosis (Fig. 3*b*). Similarly, a fusion of RARα with the promyelocytic leukemia-sequestrated repressor protein DAXX (14) was able to confer resistance to PXD101 in colony formation assays (Fig. 3*b*). These results indicate that the transactivation function of RARα is dispensable for resistance to PXD101 and that the repression function of RARα is sufficient to allow cell survival and proliferation in the presence of HDACI.

Modulators of nuclear receptor signaling often contain one or more nuclear receptor (NR) boxes, LXXLL motifs (where L is leucine and X is any amino acid), which mediate binding to the receptors. PRAME contains seven putative NR boxes (Fig. 3*d*), and it has been reported that only the most C-terminal NR motif in PRAME, LRELL, is required for binding to RARα and repression of RA signaling (9). We expressed NR box mutants of PRAME in *Ras*^{V12} MEFs and observed that all PRAME mutants allowed colony formation in 1 μM PXD101 to a similar extent, except for the C-terminal NR box mutant, LREVV (Fig. 3*d*). Because only this mutant also failed to repress RA signaling (9), this result is in keeping with the notion that PRAME allows rescue from a PXD101-mediated proliferation arrest by binding to and inhibition of RARα.

Effects of HDACI in RAR-Deficient MEFs. To investigate further the role of RAR in the cellular toxicity by HDACI we determined the sensitivity to HDACI of cells deficient for all three isoforms, RARα, β, and γ. These triple knockout RAR$^{-/-}$ MEFs (TKO MEFs) were compared with their matched controls for sensitivity to HDACI in colony formation assays. The TKO MEFs were more sensitive to HDACI than wild-type control cells because administration of low ("permissive") HDACI concentrations allowed proliferation of control MEFs, whereas the TKO MEFs were arrested (Fig. 4*a* and SI Fig. 7). Subsequently, we reconstituted RAR function in TKO MEFs by introducing the three human RAR isoforms (Fig. 4*d*). Exogenous expression of RARα rescued TKO MEFs from PXD101-induced growth arrest, but neither RARβ nor RARγ could mediate this effect (Fig. 4*b*). Expression of the RAR isoforms did not alter the induction of global histone H3 and H4 hyperacetylation by PXD101 (Fig. 4*c*).

Knockdown of PRAME Sensitizes Cells to HDACI. The tumor antigen PRAME is expressed in a variety of human cancers (15). It has been shown that knockdown of PRAME relieves repression of the RA pathway, resulting in enhanced RA signaling and decreased proliferation rates of melanoma cells in the presence of RA (9). To investigate whether endogenous PRAME expression in human tumor cells also attenuates HDACI-induced RA signaling, we used RNAi to knock down PRAME by introducing the specific short

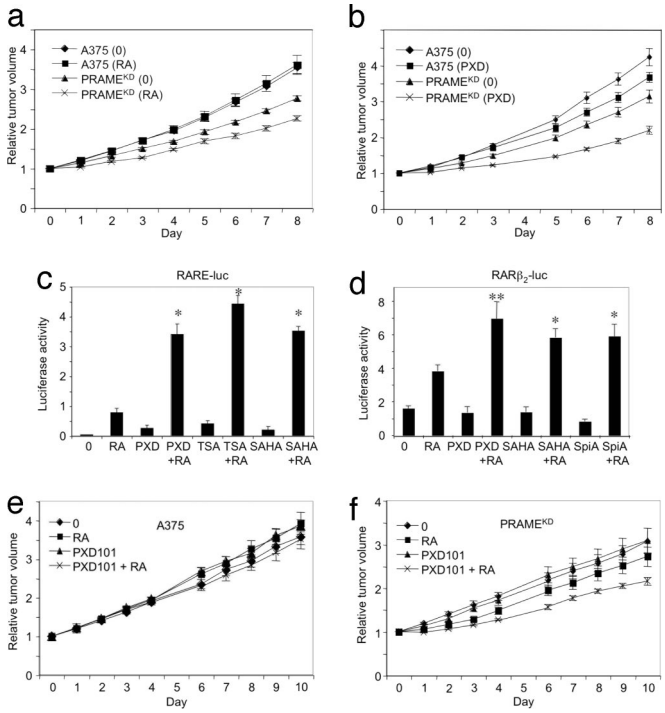

Fig. 5. Effects of knockdown of *PRAME* on sensitivity to PXD101 in mouse models. (*a* and *b*) Xenografts (s.c.) of A375 and A375-PRAME^{KD} cells. Once tumors had reached a palpable size, the mice were administered 5 mg/kg RA (*a*) or 60 mg/kg PXD101 (*b*) daily. PXD101 inhibited the growth of PRAME^{KD} tumors ($P < 0.0001$). The tumor volumes presented are relative to day 0. (*c*) U2OS cells were treated with 5 μM PXD101, 1 μM TSA, or 5 μg/ml SAHA with or without 1 μM RA, and RAR-dependent transactivation was determined by activation of the RARE3-tk-luc reporter. *F* tests were conducted to determine whether the effects of RA and HDACI were synergistic. *, $P < 0.0001$. (*d*) The *RARβ*$_2$ promoter-luc reporter was transfected into U2OS cells before treatment with 0.1 μM RA, 2 μM PXD101, 2 μM SAHA, or 20 nM spiruchostatin A. Synergy was tested and shown as *, $P < 0.0001$; **, $P < 0.005$. (*e* and *f*) Xenografts (s.c.) of A375 (*e*) and A375-PRAME^{KD} (*f*) cells. The mice were administered suboptimal doses of RA (2.5 mg/kg), PXD101 (40 mg/kg), or both daily for 7 days, and then treatment was halted. A375 tumors did not respond to these treatments. Only the combination treatment inhibited the growth of PRAME^{KD} tumors. *, $P < 0.002$.

hairpin RNA vector pRS-PRAME in human A375 melanoma cells, which express high levels of endogenous PRAME (9) (Fig. 4*e*). Knockdown of PRAME did not affect histone H3 hyperacetylation and the increase in p21 levels by PXD101. To test the effects of PRAME knockdown on RA signaling, A375 cells were cotransfected with the RARE3-tk-luc reporter and pRS-PRAME. Knockdown of PRAME enhanced PXD101-mediated RAR transactivation in a dose-dependent manner (Fig. 4*f*). To ask whether knockdown of PRAME also enhanced the antiproliferative effects of PXD101, we made derivatives of A375 with stable knockdown of endogenous PRAME, which we indicate as A375-PRAME^{KD} cells (Fig. 4*e*). A375 cell growth was inhibited by PXD101, but A375-PRAME^{KD} cells were more sensitive to PXD101 than were parental and vector control cells (Fig. 4*g*). Knockdown of PRAME also sensitized the cells to caspase-dependent apoptosis induced by PXD101, trichostatin A (TSA), and butyrate (Fig. 4*h* and SI Fig. 9).

Subsequently, we xenografted A375 and A375-PRAME^{KD} cells in nude mice to assess the *in vivo* effects of RA and PXD101. Once the tumors had reached a palpable size, the mice were administered 5 mg/kg RA or 60 mg/kg PXD101 under a daily regimen. A375-PRAME^{KD} tumors demonstrated a growth delay compared with A375 tumors and were sensitive to RA-induced growth inhibition, whereas A375 tumors were fully resistant to RA (Fig. 5*a*). Administration of PXD101 to xenografted mice resulted in a slight growth delay (13%) of A375 tumors but a substantial growth delay (30%) of A375-PRAME^{KD} tumors (Fig. 5*b*). Accordingly, the tumor doubling times of A375-PRAME^{KD} tumors in PXD101-treated mice were significantly longer than A375 tumors ($P < 0.0001$). The differential responses to PXD101 upon PRAME down-regulation is most readily explained by the function of PRAME as a negative regulator of RAR (9).

Cooperative Effects of RA and HDACI. The above findings led us to examine the effects of combination treatments of HDACI and RA *in vitro* and *in vivo*. We observed a synergistic induction of RAR transactivation when cells were treated with combinations of RA with different HDACI compared with either drug alone (Fig. 5*c* and SI Fig. 10). The activation of RA signaling by RA and HDACI was greater than the added effects of either agent alone. We therefore conclude that the activation of RA signaling by combinations of RA and HDACI is synergistic, which was confirmed by statistical analysis (Fig. 5*c* and SI Fig. 10). Similarly, the promoter of *RARβ*$_2$, a bona fide RARα target gene (16), was synergistically activated by combinations of RA plus HDACI (Fig. 5*d*). The promoter of *RARβ* is directly responsive to RA through its RARE (16), and we have shown previously that PRAME can inhibit the endogenous *RARβ*$_2$ promoter in a RA-dependent manner (9). However, a *RARβ*$_2$ promoter with a mutated RARE (M3M7-luc) was unresponsive to RA, HDACI, and the combination thereof, confirming the involvement of the RARE in these effects (SI Fig. 10). The transcriptional effects of HDACI are often mediated by SP1 sites in gene promoters, e.g., *p21* is activated by HDACI through SP1 sites in its promoter, independent of *p53* status (17). The tk minimal promoter contains two SP1 sites, and a tk-luc reporter was moderately responsive to HDACI but was not activated by RA (SI Fig. 10). However, addition of the *RARβ*$_2$ promoter to the tk-minimal promoter (*RARβ*$_2$-tk-luc) allowed for a strong response to RA and to combinations of RA and HDACI (SI Fig. 10). These experiments indicate that both RAREs and SP1 sites contributed to the synergistic responses to HDACI and RA. This finding may be explained by the interaction of RARα with HDACs and by the repression of SP1 sites by HDACs (18). Moreover, it has been demonstrated that SP1 sites can themselves function as RAREs (19).

Subsequently, we investigated the effects of combination treatments of RA and PXD101 *in vivo*. Mice with xenografted A375 and A375-PRAME^{KD} tumors were administrated RA, PXD101, or both under a daily regimen. To allow for cooperative effects to occur, we used a suboptimal dose of RA (2.5 mg/kg) and an ineffective dose of PXD101 (40 mg/kg), as determined in previous dose-response titration experiments. A375 melanoma tumors were fully resistant to both agents and continued to grow without delay, despite the treatments ($P = 0.2211$) (Fig. 5). The growth of A375-PRAME^{KD} tumors was not affected by RA or PXD101 alone. Interestingly, A375-PRAME^{KD} tumors demonstrated sensitivity to the combination of low-dose drugs and were growth-inhibited when tumors were treated with RA and PXD101 together ($P < 0.002$) (Fig. 5*f*).

Discussion

In the present work we used a functional genetic approach to gain insight into the molecular pathways targeted by HDACI that are rate-limiting for growth. The present data demonstrate that large-scale genetic screens are powerful tools to identify critical genes and pathways targeted by compounds of clinical interest. Our results provide evidence for the involvement of the RA pathway in the antiproliferative and proapoptotic effects induced by HDACI and are consistent with a model in which HDACI exert their cellular effects, at least in part, by derepression of RAR signaling through inhibition of the enzymatic activity of HDACs in the RAR repression complex. This inhibition leads to partial activation of RAR

target genes. The observed synergistic action of RA with HDACI is consistent with this model because inhibition of HDACs in the RAR repressor complex by HDACI would aid the switch from the RARα repressor function to the activator function. In agreement with this model, we found that RARα, but not RARβ or RARγ, can confer resistance to HDACI. In the absence of ligand, RARα is a strong repressor of target gene expression, whereas both RARβ and RARγ fail to repress and may even mediate ligand-independent transcriptional activation (20). Indeed, we find that RARα overexpression inhibits RA signaling and induction of RARβ (Fig. 2*c*). Thus, the finding that RARα confers resistance to HDACI is consistent with the notion that restoration of repression is required to bypass HDACI cytotoxicity. It is important to note that the reported induction of HDACI resistance by RARα and PRAME is seen at concentrations of drug that are similar to the plasma concentrations obtained in patients.

The observed synergy between RA and HDACI suggests that the antitumor effect of HDACI may be enhanced when they are combined and provides a rationale for combining these two compounds in clinical studies. Indeed, in several mouse xenograft studies involving renal cell carcinoma and neuroblastoma, synergistic tumor growth inhibition has been observed with HDACI plus retinoids (21–24).

The genetic screen was not exhaustive (only one cDNA library was used), and the cDNAs for *RARα* and *PRAME* were each detected only once. Our data therefore certainly do not rule out that HDACI have additional effects and targets and that other mechanisms of resistance exist. The observation that cells lacking all RARs still show sensitivity to HDACI demonstrates that RAR repression is required for HDACI resistance but at the same time underscores that other targets also mediate cytotoxic effects of HDACI. Consistent with this observation, several studies have demonstrated that specific genes can mediate HDACI-induced cytotoxicity, including the ROS-scavenger thioredoxin in solid tumor cells and the death receptor pathway components Fas and TNF-related apoptosis-inducing ligand in leukemias (25–27). In addition, the failure to activate G_2/M cell cycle checkpoints that are available in normal cells and transcription-independent mechanisms in mitosis are involved in the mechanisms of action of HDACI (28, 29).

Cutaneous T cell lymphomas (CTCL) are malignancies of T cells appearing as skin lesions, and they have shown responsiveness to HDACI in clinical trials (30). In CTCL patients, retinoid X receptor (RXR)-selective retinoids (rexinoids) have proven effective for the treatment of refractory disease (31). Recently, the first CTCL patient treated with a combination of HDACI and a rexinoid has been reported, and this patient showed massive tumor necrosis of lymphoma lesions and no new lesions after discontinuation of treatment (32). The mechanism of the remarkable antitumor action of rexinoid and HDACI therapy in this patient has not been clarified. RXR is the obligate heterodimerization partner of RAR and is required for DNA binding, repression, and activation of gene transcription. Based on our genetic data, it can be hypothesized that the clinical utility of the combination of HDACI and rexinoids could be based on their effects on RAR/RXR signaling.

Materials and Methods

Plasmid Construction, Reagents, and Antibodies. RAR and PRAME expression constructs were generated by cloning the respective wild-type and mutant human RAR and PRAME cDNAs into the cytomegalovirus-driven expression vectors pSG5 or pcDNA3.1 and into the retroviral vectors pMX, pMSCV, or pBabe-puro. RAR wild-type and mutant constructs and the luciferase reporters were kindly provided by H. Stunnenberg (Nijmegen, The Netherlands) and H. de Thé (Paris, France). The *RARβ$_2$*-luc (also termed R140-luc) and M3M7-luc reporters were as described (33), and the *RARβ$_2$*-tk-luc reporter was made by cloning the *RARβ$_2$* promoter in a preexisting tk-luc plasmid. The RAR-Rac mutation has a 29-aa deletion in the C-terminal part of the ligand-binding domain comprising the AF-2 AD core helix H12. The PRAME mutants were made by site-directed mutagenesis PCR and were subsequently cloned into pMX. pRS-PRAME was as described (9). The K562 erythroleukemia retroviral cDNA library was a gift from E. Koh and G. Daley (Cambridge, MA). All-*trans*-retinoic acid (ATRA, RA), TSA, valproic acid, butyrate, and MS-275 were purchased from Sigma (St. Louis, MO). Suberoylanilide hydroxamic acid (SAHA) was purchased from Alexis (San Diego, CA). PXD101 was a gift from Topotarget/Prolifix Ltd. (Abingdon, U.K.), and spiruchostatin A was a gift from A. Ganesan and G. Packham (University of Southampton, U.K.). Anti-PRAME affinity-purified antibodies were generated by immunizing rabbits with peptides FPEPEAAQPMTKKRKVDG and CGDRTFYDPEPIL. Antibodies against RARα (C-20), RARβ (C-19), RARγ (C-20), p21 (F5), GFP (FL), and CDK4 (C-22) were from Santa Cruz Biotechnologies (Santa Cruz, CA). Anti-acetyl H3 was from Serotec (Raleigh, NC), and anti-acetyl H4 was from Transduction Laboratories (Lexington, KY).

Cell Culture, Genetic Screen, and Colony Formation Assays. All cells were cultured in DMEM supplemented with 10% FCS, except for A2780 cells, which were grown in RPMI medium 1640 supplemented with 10% FCS. Phoenix packaging cells were transfected with retroviral plasmids to generate ecotropic retroviruses. *p53$^{-/-}$* MEFs were infected with pBabe-puro-*RAS^{V12}* retrovirus and selected for puromycin resistance. The resulting *RAS^{V12}* MEFs were infected with library retroviral supernatants and replated at a cell density of 5×10^4 cells per 10-cm tissue culture dish 48 h after infection. PXD101 (1 μM) was added to the medium 16 h after plating, and fresh medium with PXD101 was added every 3rd day. Wild-type Moloney virus infection and mobilization of proviral inserts for subsequent confirmatory infection rounds were done as described (34). Retroviral inserts were retrieved by PCR, cloned, and sequenced. For colony formation assays, the cells were transduced with retroviral supernatants followed by plating and treatment with HDACI as described for the screen. Colony formation assays were repeated two to four times in duplicate. TKO MEFs were seeded at 10^5 cells per 10-cm dish and treated with 0.25 μM PXD101. Dishes were stained with Coomassie blue 14–18 days after plating.

Transfections and Reporter Assays. Transfections were carried out by using calcium phosphate precipitation, except for A375 cells, which were transfected by using the Lipofectamine 2000 reagent (Invitrogen, Carlsbad, CA). Reporter assays with experimentally added RA were done in DMEM supplemented with charcoal-stripped FCS (HyClone, Logan, UT), and reporter assays without experimentally added RA were done in standard FCS. In reporter assays, 0.5 μg of reporter-luciferase was cotransfected with 10 ng of cytomegalovirus-*Renilla* and 3 μg of the indicated DNA (pSG5-RARα, pcDNA3-PRAME). RA and HDACI were added 24 h after transfection, and assays were done 48 h after transfection. In RNAi experiments, PXD101 was added 72 h after transfection, and the assays were done 96 h after transfection. Reporter assays were done at least three times in triplicate. Normalized luciferase activities shown represent ratios between luciferase values and *Renilla* internal control values and were measured by using the dual reporter luciferase assay system (Promega, Madison, WI).

Western Blotting and Apoptosis Assays. Cells were lysed in radioimmunoprecipitation assay buffer (50 mM Tris, pH 8.0/150 mM NaCl/1% Nonidet P-40/0.5% deoxycholic acid/0.1% SDS) supplemented with protease inhibitors (Complete; Roche, Indianapolis, IN) and 0.2 nM PMSF, and proteins were separated on SDS/10–14% polyacrylamide gels. Proteins were transferred to polyvinylidine difluoride membranes (Immobilon P; Millipore, Billerica, MA) and Western blots were probed with the indicated antibodies.

To measure apoptosis, cells were plated at a density of 10,000 cells per well in 96-well plates and cultured for 24 h; HDACI were added, and the cells were cultured for another 24 h. The cells were lysed, and apoptosis was detected by using the Apo-ONE assay (Promega), which quantifies caspase 3/7-specific cleavage of a peptide-based substrate into a fluorescent product.

Mouse Tumor Xenografts. Athymic nude mice (female CD1 nu/nu from Charles River Laboratories, Wilmington, MA) were injected s.c. with 10^7 cells bilaterally into the axial regions. Each mouse received A375-PRAME^{KD} cells in its left flank and control A375 cells in its right flank. Mice were randomized into treatment groups (six animals per group) and treated daily for 7 days with RA (orally in 10% ethanol in sunflower oil) or with PXD101 (i.p., prepared as for the clinical formulation in L-arginine). Treatment was started when the tumors were $\pm$0.5-cm mean diameter. Tumors were measured with calipers, and the volume was calculated from the mean of 2 diameters ($d^3 \times \pi/6$). Results shown are the relative tumor volumes defined as the tumor volume divided by the volume on day 0. We have reported relative tumor volumes to correct for the variations in the initial tumor sizes. The growth rates of the tumors were the same regardless of starting size. Tumor doubling time was estimated for each mouse as the time taken for the tumor to reach twice the initial starting volume. The pRS vector that was used to generate A375-PRAME^{KD} cells is a self-inactivating retroviral vector, to prevent reactivation and spreading of virus (35).

Statistical Analysis. Data are presented as means $\pm$ SD. Two-sample *t* tests were used to test differences between cell lines or drug treatments, and *F* tests were conducted to test for synergy. To determine whether there was synergy, we tested whether the effect of the addition of two drugs was greater than the added effects of the two individual drugs. Significant differences in tumor doubling times were determined by analysis of variance. Statistical analysis was carried out in R (2.5.0) software.

We thank Henk Stunnenberg and Hugues de Thé for plasmid constructs, Topotarget, Ltd. for PXD101, Drs. A. Ganesan and G. Packham for spiruchostatin A, George Daley and Eugene Koh for the retroviral cDNA expression library, and Nicola Armstrong for statistical analysis. This work was supported by grants from the Centre for Biomedical Genetics, the Dutch Cancer Society, and Cancer Research United Kingdom Program Grants A2662 and A4745.

1. Roth SY, Denu JM, Allis CD (2001) *Annu Rev Biochem* 70:81–120.
2. Johnstone RW (2002) *Nat Rev Drug Discov* 1:287–299.
3. Minucci S, Pelicci PG (2006) *Nat Rev Cancer* 6:38–51.
4. Kelly WK, O'Connor OA, Krug LM, Chiao JH, Heaney M, Curley T, MacGregore-Cortelli B, Tong W, Secrist JP, Schwartz L, *et al*. (2005) *J Clin Oncol* 23:3923–3931.
5. Van Lint C, Emiliani S, Verdin E (1996) *Gene Expression* 5:245–253.
6. Peart MJ, Smyth GK, van Laar RK, Bowtell DD, Richon VM, Marks PA, Holloway AJ, Johnstone RW (2005) *Proc Natl Acad Sci USA* 102:3697–3702.
7. Ikeda H, Lethe B, Lehmann F, van Baren N, Baurain JF, de Smet C, Chambost H, Vitale M, Moretta A, Boon T, Coulie PG (1997) *Immunity* 6:199–208.
8. Glass CK, Rosenfeld MG (2000) *Genes Dev* 14:121–141.
9. Epping MT, Wang L, Edel MJ, Carlee L, Hernandez M, Bernards R (2005) *Cell* 122:835–847.
10. Yurek-George A, Habens F, Brimmell M, Packham G, Ganesan A (2004) *J Am Chem Soc* 126:1030–1031.
11. McKenna NJ, O'Malley BW (2002) *Cell* 108:465–474.
12. Freedman LP (1999) *Cell* 97:5–8.
13. Renaud JP, Rochel N, Ruff M, Vivat V, Chambon P, Gronemeyer H, Moras D (1995) *Nature* 378:681–689.
14. Li H, Leo C, Zhu J, Wu X, O'Neil J, Park EJ, Chen JD (2000) *Mol Cell Biol* 20:1784–1796.
15. Epping MT, Bernards R (2006) *Cancer Res* 66:10639–10642.
16. de Thé H, Vivanco-Ruiz MM, Tiollais P, Stunnenberg H, Dejean A (1990) *Nature* 343:177–180.
17. Sowa Y, Orita T, Minamikawa S, Nakano K, Mizuno T, Nomura H, Sakai T (1997) *Biochem Biophys Res Commun* 241:142–150.
18. Doetzlhofer A, Rotheneder H, Lagger G, Koranda M, Kurtev V, Brosch G, Wintersberger E, Seiser C (1999) *Mol Cell Biol* 19:5504–5511.
19. Suzuki Y, Shimada J, Shudo K, Matsumura M, Crippa MP, Kojima S (1999) *Blood* 93:4264–4276.
20. Hauksdottir H, Farboud B, Privalsky ML (2003) *Mol Endocrinol* 17:373–385.
21. Wang XF, Qian DZ, Ren M, Kato Y, Wei Y, Zhang L, Fansler Z, Clark D, Nakanishi O, Pili R (2005) *Clin Cancer Res* 11:3535–3542.
22. Trus MR, Yang L, Suarez Saiz F, Bordeleau L, Jurisica I, Minden MD (2005) *Leukemia* 19:1161–1168.
23. Coffey DC, Kutko MC, Glick RD, Butler LM, Heller G, Rifkind RA, Marks PA, Richon VM, La Quaglia MP (2001) *Cancer Res* 61:3591–3594.
24. Touma SE, Goldberg JS, Moench P, Guo X, Tickoo SK, Gudas LJ, Nanus DM (2005) *Clin Cancer Res* 11:3558–3566.
25. Ungerstedt JS, Sowa Y, Xu WS, Shao Y, Dokmanovic M, Perez G, Ngo L, Holmgren A, Jiang X, Marks PA (2005) *Proc Natl Acad Sci USA* 102:673–678.
26. Nebbioso A, Clarke N, Voltz E, Germain E, Ambrosino C, Bontempo P, Alvarez R, Schiavone EM, Ferrara F, Bresciani F, *et al*. (2005) *Nat Med* 11:77–84.
27. Insinga A, Monestiroli S, Ronzoni S, Gelmetti V, Marchesi F, Viale A, Altucci L, Nervi C, Minucci S, Pelicci PG (2005) *Nat Med* 11:71–76.
28. Li Y, Kao GD, Garcia BA, Shabanowitz J, Hunt DF, Qin J, Phelan C, Lazar MA (2006) *Genes Dev* 20:2566–2579.
29. Warrener R, Beamish H, Burgess A, Waterhouse NJ, Giles N, Fairlie D, Gabrielli B (2003) *FASEB J* 17:1550–1552.
30. Olsen EA, Kim YH, Kuzel TM, Pacheco TR, Foss FM, Parker S, Frankel SR, Chen C, Ricker JL, Marie Arduino J, Duvic M (2007) *J Clin Oncol* 25:3109–3115.
31. Duvic M, Hymes K, Heald P, Breneman D, Martin AG, Myskowski P, Crowley C, Yocum RC, Bexarotene Worldwide Study Group (2001) *J Clin Oncol* 19:2456–2471.
32. Steinhoff M, Beyer M, Roewert-Huber J, Lukowsky A, Assaf C, Sterry W (2007) *J Am Acad Dermatol*, in press.
33. Vivanco Ruiz MM, Bugge TH, Hirschmann P, Stunnenberg HG (1991) *EMBO J* 10:3829–3838.
34. Jacobs JJ, Keblusek P, Robanus-Maandag E, Kristel P, Lingbeek M, Nederlof PM, van Welsem T, van de Vijver MJ, Koh EY, Daley GQ, van Lohuizen M (2000) *Nat Genet* 26:291–299.
35. Brummelkamp TR, Bernards R, Agami R (2002) *Cancer Cell* 2:243–247.